

Fracture Behavior of Silicon Nitride-silicon Carbide-boron Nitride Multi-layer Composites with Different Layer Thickness

Byoung-Uk Cho**, Dong-Soo Park^{†*} and Hong-Chae Park**

Ceramic Materials Group, Korea Institute of Machinery and Materials, Kyong-Nam 641-010, Korea
Department of Materials Science and Engineering, Pusan National University, Pusan 609-735, Korea
(Received June 14, 2002; Accepted July 19, 2002)

ABSTRACT

Multi-layer composites consisting of silicon nitride, silicon nitride-silicon carbide and boron nitride-alumina layers were prepared by stacking the corresponding ceramic tapes. The composites demonstrated self-diagnostic capability and non-catastrophic failure behavior. The composites consisting of many thin layers exhibited high strength and stepwise increase of the electrical resistance during the flexure test. The strength of the composite with too thick silicon nitride layers was low and the electrical resistance was abruptly increased to the detection limit of the digital multi-meter during the test. An extensive crack branching was observed in the weak (BN + Al₂O₃) layer.

Key words : Multi-layer composite, Self-diagnostic, Non-catastrophic failure, Electrical resistance

1. Introduction

There have been a lot of efforts to develop ceramic composites showing non-catastrophic failure behavior without using the expensive ceramic fibers.¹⁻⁵⁾ In most cases, weak boundaries were incorporated in the ceramic composites to deflect the crack. The multi-layer composites as well as the fibrous monolithic ceramics successfully demonstrated non-catastrophic failure behavior.¹⁻⁴⁾ Clegg *et al.*, developed SiC/C multi-layer composite that had multiple deflections in the load-displacement diagram as well as in the crack propagation path.¹⁾ The SiC/C multi-layer composite exhibited higher flexural strength as well as much larger fracture energy than the monolithic SiC. Philips *et al.* reported that the fracture energy was increased as the number of layers per the sample thickness was increased.²⁾ They ascribed the increased fracture energy to the improved strength of the SiC layer according to the decreased thickness. Liu and Hsu prepared Si₃N₄/BN multi-layer composite and reported its non-catastrophic fracture behavior similar to that of the above SiC/C multi-layer composite.³⁾ They reported that the layer structure parameters including the layer thickness, the interfacial layer toughness and the layer strength needed optimizing for further improvement of the fracture toughness and strength of the multi-layer composite.

Self-diagnosis is capability of detecting damage or fracture. Shin and Matsubara reported that electrical resis-

tance of the carbon particle-glass-fiber-reinforced plastics was almost linearly increased as the tensile strain was increased.⁶⁾ They also measured the electrical resistance of SiC fiber reinforced Si₃N₄ composites added with tungsten fiber or TiN particles. They reported that the electrical resistance of those composites was increased during the flexure tests.

In this study, we prepared four kinds of ceramic tapes; silicon nitride, silicon nitride + 20 wt% SiC whiskers, boron nitride-alumina and silicon nitride + 20 wt% SiC particles. By changing the stacking sequence, multi-layer composites with different layer thickness were prepared. Fracture behaviors of the composites were studied using the load-displacement curve and variation of electrical resistance during the three point flexure tests.

2. Experimental Procedure

Four kinds of ceramic tapes were prepared using the slurries containing 1) 92 wt% α -Si₃N₄ powder (SN E10, Ube Industries Ltd., Yamaguchi, Japan)-6 wt% Y₂O₃ (H. C. Starck Co., Berlin, Germany)-2 wt% Al₂O₃ (AKP-30, Sumitomo Chemical Co., Osaka, Japan), 2) 72 wt% α -Si₃N₄ powder -6 wt% Y₂O₃ -2 wt% Al₂O₃-20 wt% SiC whiskers (TWS-400, Tokai Carbon, Tokyo, Japan), 3) 88 wt% BN (A01, H. C. Starck Co.)-12 wt% Al₂O₃ and 4) 72 wt% α -Si₃N₄ -6 wt% Y₂O₃ -2 wt% Al₂O₃ 20 wt% β -SiC powder (UF, Ividen Co., Tokyo, Japan). Detailed procedure for the slurry preparation was provided in the previous report.⁷⁾ The tapes were cut into sheets with 35 × 35 mm² dimensions. Sheets prepared from the slurries 1), 2), 3) and 4) are labeled as sheets A, B, C and D, respectively. Four kinds of samples were labeled as 1 W, 3 W, 5 W and 1 P depending on the stacking

[†]Corresponding author : Dong-Soo Park

E-mail : pds1590@kmail.kimm.re.kr

Tel : +82-55-280-3345 Fax : +82-55-280-3399

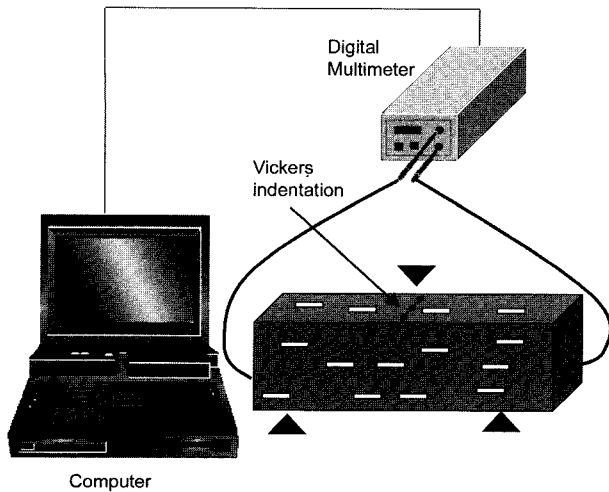


Fig. 1. Schematic diagram for the flexure bar.

sequence of the sheets. The stacking sequences of samples 1 W, 3 W, 5 W and 1 P were A-B-A-C, 3A-B-3A-C, 5A-B-5A-C and A-D-A-C, respectively. The number in front of the sheet name represents how many sheets were repeatedly stacked. After stacking, lamination was performed at 318 K under 50 MPa using a lever press. Binder burnout was carried out at 873 K for 10 h in a flowing air environment.

After binder burnout, the samples were hot pressed using BN-coated graphite mould and punch in a flowing nitrogen environment. Hot pressing was performed at 2073 K under 30 MPa. Hot pressed plates were sliced into bars with $3 \times 4 \times 34 \text{ mm}^3$ dimensions. Those bars were ground and polished with $1 \mu\text{m}$ diamond slurry. Three Vickers indentations were performed on the surface of the bar that was subjected to tensile stress during the flexure test. A schematic diagram for the flexure bar is shown in Fig. 1. Electrical contacts were made on both ends of the flexure bar ($3 \times 4 \text{ mm}^2$ faces) and they were connected to a digital multi-meter (Model 7561, Yokogawa Electric Co., Tokyo, Japan) for measuring electrical resistance. Measured electrical resistance data were stored in a computer. The data-sampling interval was 100 ms. Three point flexure tests were performed using 20 mm span. The cross-head speed was 0.5 mm/min. During the flexure test, the load-deflection data were also obtained.

3 Results and Discussion

Fig. 2 shows electrical resistance values of the flexure bars with the same dimensions ($3 \times 4 \times 31.5 \text{ mm}^3$). Thickness of the layers corresponding to the sheets A, B, C and D were about $100 \mu\text{m}$, $20 \mu\text{m}$, $80 \mu\text{m}$ and $20 \mu\text{m}$, respectively. Among those four kinds of sheets, only sheets B and D containing SiC were electrically conductive and others were electrically insulators. Bend bar from sample 1 W had 9 or 10 electrically conductive layers while bend bars from samples 3 W and 5 W had 4 or 5 and 2 or 3 electrically conductive layers, respectively. Electrical resistance was increased

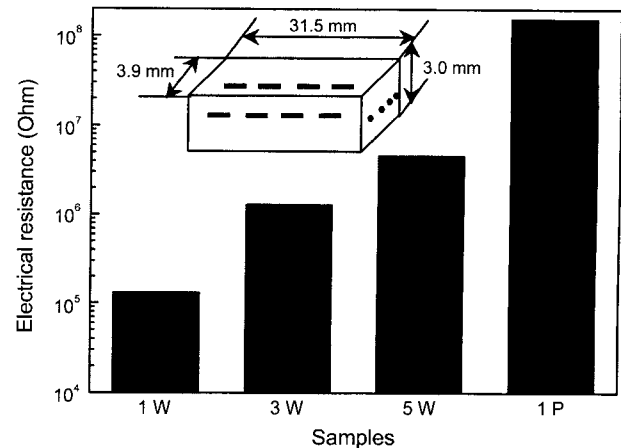


Fig. 2. Electrical resistance of the bend bars.

as the number of the electrically conductive layers was decreased. Further analysis reveals that electrical resistance of the sample per the electrically conductive layer (measured electrical resistance/the number of electrically conductive layers within the flexure bar) was increased as the number of electrically conductive layers was decreased. Comparison of samples 1 W and 1 P shows that the SiC whiskers were more effective for providing electrically conductive path than the SiC particles. McLachian *et al.*, reported that much smaller amount of the short fibers with the high aspect ratio were needed for the impingement among themselves than the particles with equi-axial shapes.⁸⁾

Fig. 3(a)-(d) show the load-displacement curves of the samples during the flexure tests. All the samples experienced at least two load drops during the flexure tests, indicating that non-catastrophic failure took place. The number of load drops was the largest for sample 1 W. According to Philipps *et al.*, the load drop represented failure and debonding of layers and large load drop often corresponded to the simultaneous failure of multiple layers.²⁾ Although sample 1 W had almost the same number of the weak layers as sample 1 P, it experienced larger number of the load drops than from sample 1 P. One possible reason why the two samples experienced different numbers of the load drops is that the loads needed to fracture the layers were more uniform for sample 1 W than for sample 1 P. The number of load drops was smaller for samples 3 W and 5 W than for sample 1 W in part due to the fact that they had fewer weak layers than sample 1 W. The flexural strengths of samples 1 W, 3 W, 5 W and 1 P were 637.7, 250.5, 213.4 and 352.1 MPa, respectively. It is interesting to note that sample 1 W was stronger than sample 3 W or sample 5 W although larger number of the weak layers were involved in sample 1 W than in either of the other two samples. The strength of sample 1 W was higher than that of sample 1 P, suggesting that the aligned SiC whiskers were better for high strength of the composite than the SiC particles. It is understood from Fig. 3(a)-(d) that the strong layers should not be too

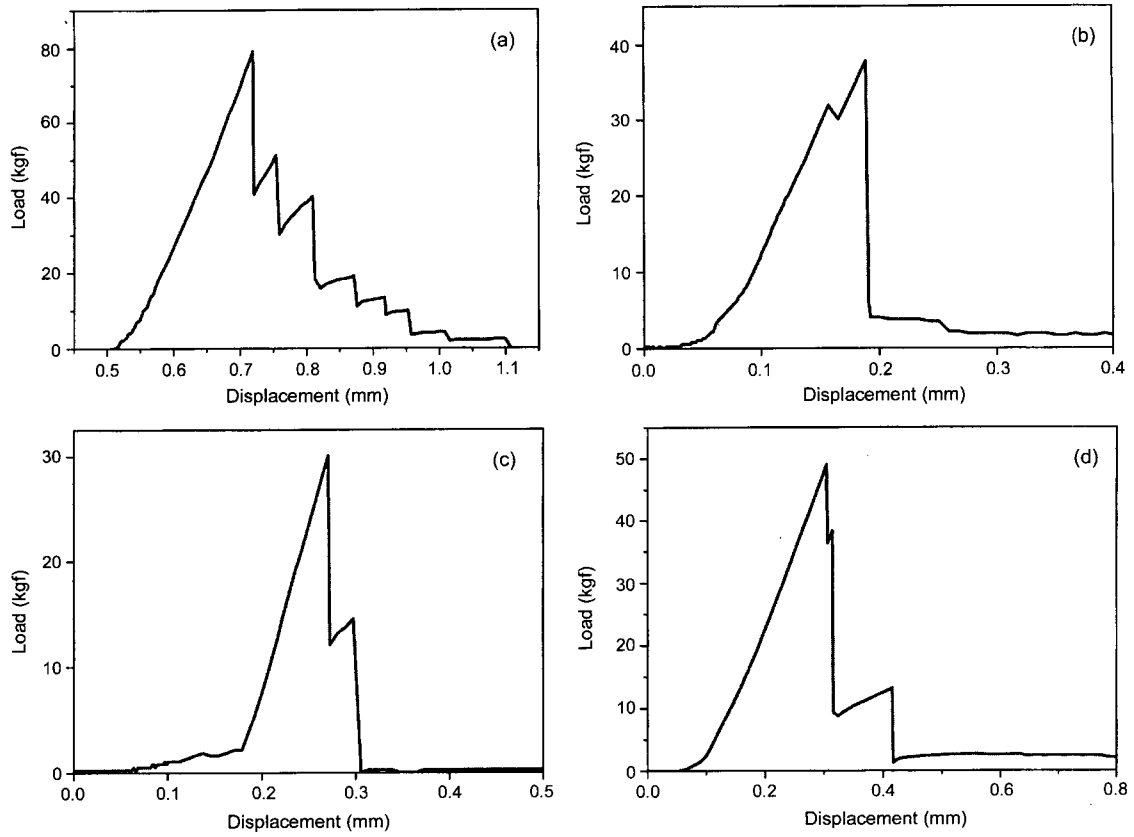


Fig. 3. Load-displacement curves of the samples obtained from the flexure tests; (a) sample 1 W, (b) sample 3 W, (c) sample 5 W and (d) sample 1 P.

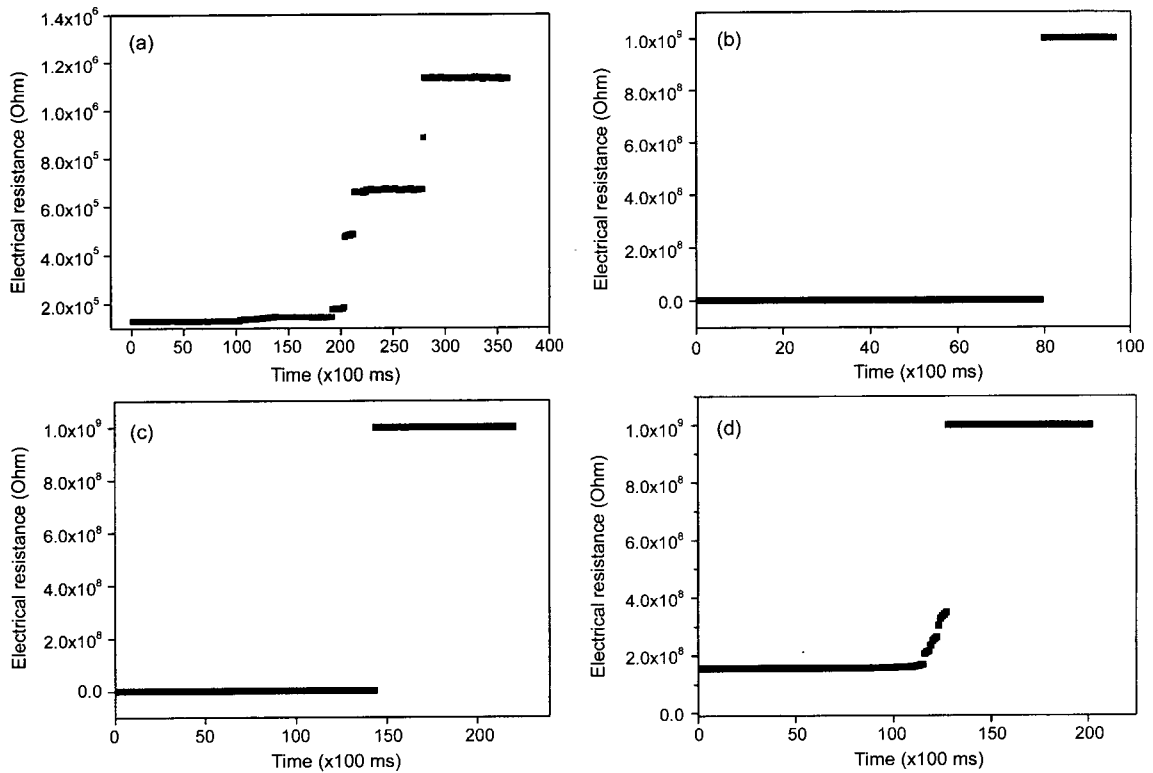


Fig. 4. Variations of electrical resistance of the bend bars prepared from samples (a) 1 W, (b) 3 W, (c) 5 W and (d) 1 P.

thick for high strength of the composite as well as for non-catastrophic failure behavior.

Fig. 4(a)-(d) show variations of the electrical resistance of the samples during the flexure tests. Sample 1 W exhibited stepwise increase of the electrical resistance during the test. The number of the steps in Fig. 4(a) was smaller than that of load drops in Fig. 3(a). In other words, each stepwise increase of the electrical resistance did not correspond to fracture of the layers. It is probable that the electricity was still conducting even after a single sharp crack cut the SiC whisker unless there was a sufficient gap between the cut surfaces of the whisker. Sample 3 W and sample 5 W exhibited abrupt disconnection of electricity during the flexure tests. Sample 1 P showed a gradual increase of the electrical resistance at the beginning of loading. However, the electrical resistance soon got to the maximum detection limit of the digital multimeter. Since the initial electrical resistance of sample 1 P was as high as 1.56×10^8 ohm, fracture of a few layers with the SiC particles easily increased the electrical resistance to 1×10^9 ohm that is the detection limit of the digital multimeter.

Fig. 5(a)-(d) show side surfaces of the samples after fracture. Sample 1 W showed small crack deflections at the

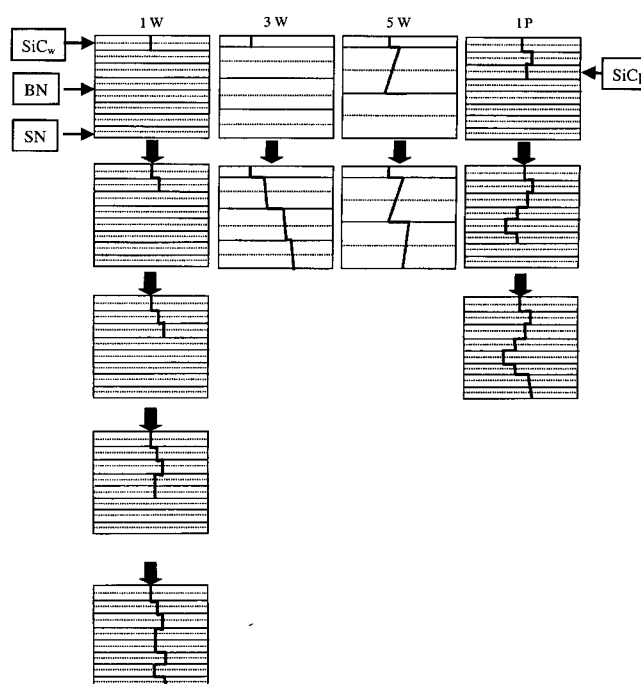


Fig. 6. Schematic diagrams for the crack propagation within the bend bars during the flexure test.

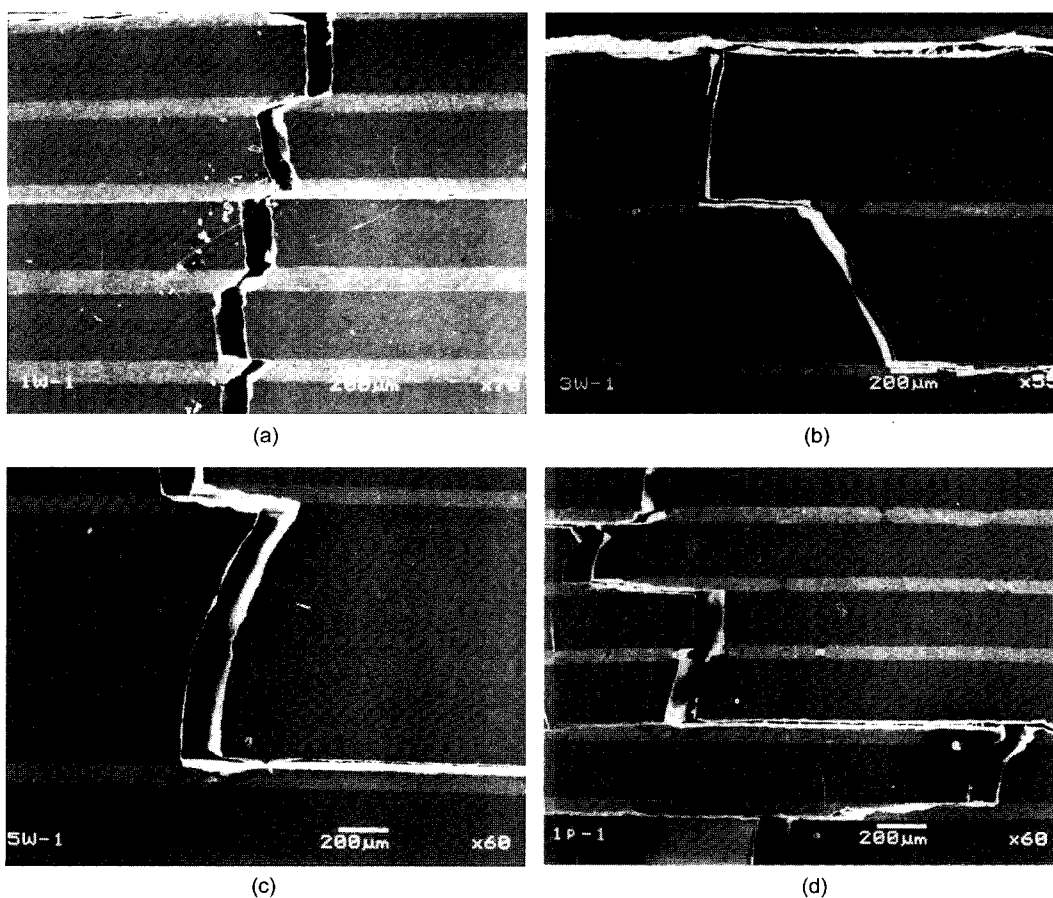
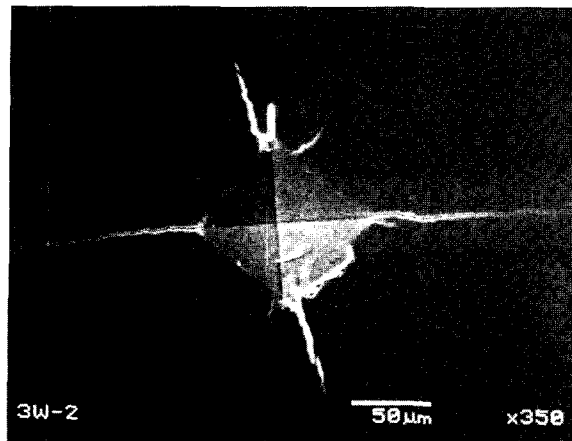
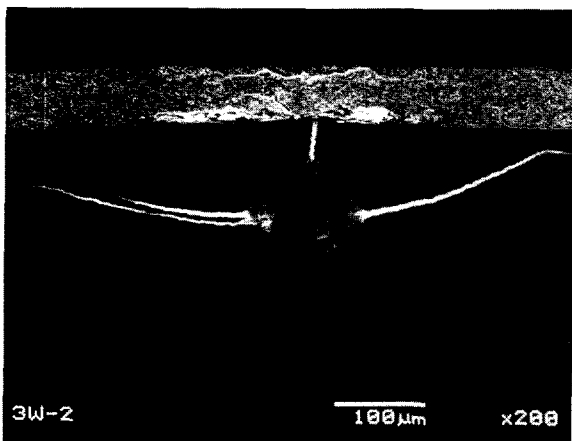


Fig. 5. SEM micrographs of bend bars after the flexure; bend bars from (a) sample 1 W, (b) sample 3 W, (c) sample 5 W and (d) sample 1 P.

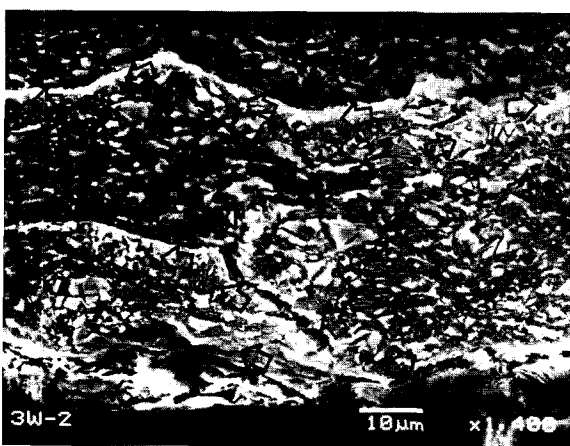
weak layers. Sample 3 W and sample 5 W showed significant crack deflections at some of the weak layers. Sample 1 P also showed the crack deflected at the weak layers. The



(a)



(b)



(c)

Fig. 7. Cracks generated by Vickers indentation under 98 N; (a) indentation performed at the center of silicon nitride-20 wt% SiC whisker layer, (b) indentation performed within silicon nitride layer about 100 μm off the interface with BN-12 wt% Al_2O_3 layer and (c) the crack within BN-12 wt% Al_2O_3 layer at higher magnification.

number of the crack deflection observed from the micrographs was not the same as that of the load drops of the load-deflection curve. Fig. 6 shows schematic diagrams for the crack propagation during the flexure tests of the samples. One load-drop in the load-deflection curve might involve more than one crack deflection as well as fracture of multiple layers.

Fig. 7(a) and (b) show how the cracks generated by Vickers indentation under 98 N load propagated depending on the position of indentation. Fig. 7(a) shows that the crack parallel to the interface was longer than the crack perpendicular to it. Since the SiC whisker has higher thermal expansion coefficient than silicon nitride, a compressive thermal residual stress was present within the silicon nitride layer as previously reported by Choi *et al.*⁹⁾ The compressive residual stress suppressed crack propagation perpendicular to the interface. Fig. 7(b) shows the cracks generated by Vickers indentation within silicon nitride layer. The indentation was performed about 100 μm off the interface with the weak layer that consisted of BN and Al_2O_3 . The crack parallel to the interface was very long and curved toward the interface. Higher magnification of the weak layer reveals that there were numerous microcracks parallel to the interface (Fig. 7(c)). The weak layer was suspected to have much lower Young's modulus due to those microcracks than silicon nitride layer. Lardner *et al.*, reported that the indentation cracks near the interface of the materials with sufficiently different Young's moduli propagated toward the interface.¹⁰⁾ Fig. 7(c) also shows that extensive crack branching occurred and the crack eventually stopped its propagation in through-thickness direction.

4. Summary

By using silicon nitride/silicon nitride-silicon carbide/boron nitride multi-layer composites, multi-layer composites exhibiting self-diagnostic capability and non-catastrophic failure behavior were fabricated. The SiC whiskers were more effective for improving the flexural strength as well as for reducing the electrical resistance than the SiC particles. The composite with thick silicon nitride layers had low strength and exhibited an abrupt increase of the electrical resistance during the flexure test. The indentation cracks in the silicon nitride layer near the interface with the weak layer consisting of BN and Al_2O_3 propagated toward the interface. Extensive crack branching was observed while the crack propagated within the weak layer.

REFERENCES

1. W. J. Klegg, K. Kendall, N. McN. Alford, T. W. Button and J. D. Birchall, "A Simple Way to Make Tough Ceramics," *Nature*, **347** 455-57 (1990).
2. A. J. Philipps, W. J. Clegg and T. W. Clyne, "Fracture Behavior of Ceramic laminates in Bending-II. Comparison of Model Predictions with Experimental Data," *Acta Met-*

- all. Mater.*, **41** [3] 819-27 (1993).
3. H. Liu and S. M. Hsu, "Fracture Behavior of Multilayer Silicon Nitride/Boron Nitride Ceramics," *J. Am. Ceram. Soc.*, **79** [9] 2452-57 (1996).
 4. D. B. Marshall, P. E. D. Morgan and R. M. Housley, "Debonding in Multilayered Composites of Zirconia and LaPO_4 ," *J. Am. Ceram. Soc.*, **80** [7] 1677-83 (1997).
 5. S. Baskaran and J. W. Halloran, "Fibrous Monolith Ceramics: II, Flexural Strength and Fracture Behavior of the Silicon Carbide/Graphite System," *J. Am. Ceram. Soc.*, **76** [9] 2217-24 (1993).
 6. S.-G. Shin and H. Matsubara, "Damage Detection in Fiber Reinforced Composites Containing Electrically Conductive Phases," *Kor. J. Ceram.*, **6** [2] 201-05 (2000).
 7. D.-S. Park, H.-D. Kim, B.-D. Han, T.-W. Roh, C. Park, B.-W. Cho and H.-C. Park, "Variation of Electrical Resistance during Fracture of Silicon Nitride-silicon Carbide Whisker-Boron Nitride Laminate Composite," *J. Mater. Sci. Lett.* (in print).
 8. D. S. McLachlan, M. Blaszkiewicz and R. E. Newham, "Electrical Resistivity of Composites," *J. Am. Ceram. Soc.*, **73** [8] 2187-203 (1990).
 9. B.-J. Choi, Y.-H. Koh and H.-E. Kim, "Mechanical Properties of Si_3N_4 -SiC Three-layer Composite Materials," *J. Am. Ceram. Soc.*, **81** [10] 2725-28 (1998).
 10. T. J. Lardner, J. E. Ritter, M. L. Shiao and M. R. Lin, "Behavior of Indentation Cracks near Free Surfaces and Interfaces," *Int. J. Fracture*, **44** 133-43 (1990).